Biochimica et Biophysica Acta 810 (1985) 33–48
Elsevier

BBA 41853

Temperature and detection-wavelength dependence of the picosecond electron-transfer kinetics measured in *Rhodopseudomonas sphaeroides* reaction centers. Resolution of new spectral and kinetic components in the primary charge-separation process

Christine Kirmaier [a], Dewey Holten [a] and William W. Parson [b]

[a] *Department of Chemistry, Washington University, St. Louis, MO 63130, and* [b] *Department of Biochemistry, University of Washington, Seattle, WA 98195 (U.S.A.)*

(Received April 10th, 1985)
(Revised manuscript received July 15th, 1985)

Key words: Bacterial photosynthesis; Reaction center; Picosecond spectroscopy; Electron transfer; Charge separation; (*Rps. sphaeroides*)

We have examined the temperature dependence of the rate of electron transfer to ubiquinone from the bacteriopheophytin (BPh) that serves as an initial electron acceptor (I) in reaction centers of *Rhodopseudomonas sphaeroides*. The kinetics were measured from the decay of the 665-nm absorption band of the reduced BPh (BPh^- or I^-) and from the recovery of the BPh band at 545 nm, following excitation of reaction centers in polyvinyl alcohol films with 30-ps flashes. The measured time constant decreases from 229 ± 25 ps at 295 K to 97 ± 8 ps near 100 K and then remains constant down to 5 K. The temperature dependence of the kinetics can be rationalized on the assumption that the reaction results in changes in the frequencies of numerous low-energy nuclear (vibrational) modes of the electron carriers and/or the protein. The kinetics measured in the absorption bands near 765 and 795 nm show essentially the same temperature dependence as those measured at 545 or 665 nm, but the time constants vary with detection wavelength. The time constant measured in the 795-nm region (70 ± 10 ps at 5 and 76 K) is shorter than that seen in the absorption bands of the BPh; the time constant measured at 758 nm is longer. Time constants measured with reaction centers in solution at 288 K also vary with the detection wavelength. These results can be explained on the assumption that the absorption changes measured at some wavelengths reflect nuclear relaxations rather than electron transfer. The absorption changes at 795 nm probably reflect a relaxation of the bacteriochlorophyll molecules that are near neighbors of the BPh and the primary electron donor (P). Those near 530 and 755 nm probably are due to the second BPh molecule, which does not appear to undergo oxidation or reduction.

Introduction

In *Rps. sphaeroides* reaction centers, excitation produces the excited singlet state (P*) of the primary electron donor (P), a complex involving two of the four bacteriochlorophyll (BChl) molecules [1]. In 4–7 ps [2–4] an electron from P* arrives on an early electron acceptor I [2–13], thought to be a complex of a bacteriopheophytin (BPh) and one of two additional BChls [11,13–17]. Previous studies have indicated that the electron is transferred from I^- to a molecule of ubiquinone

Abbreviations: P, a complex of bacteriochlorophylls (BChl); I, a complex thought to consist of a BChl and a bacteriopheophytin (BPh); Q, a reaction-center quinone.

(Q_A) with a time constant of approx. 200 ps at room temperature [2–11,18–20]. The roles of the fourth BChl and second BPh are not understood.

In the present article, we first reexamine the temperature dependence of the electron transfer reaction $P^+I^- \rightarrow P^+Q_A^-$ in *Rps. sphaeroides* reaction centers. We have investigated the temperature dependence in detail between 5 K and 295 K in polyvinyl alcohol films. Our results agree in some respects and disagree in other respects with earlier, less extensive studies of the temperature dependence of this reaction [19,20]. We discuss the new results in terms of recent theories of electron transfer. Our new results also demonstrate an unexpected detection-wavelength dependence of the observed kinetics. This finding must be taken into account in discussing the rate of electron transfer, and the molecular aspects of the primary events in general. Analysis of the data indicates the possible importance of nuclear motions of the pigments and protein on the transient spectra and kinetics.

In a subsequent article [21] we discuss the temperature dependence of the ground-state and transient-state spectra of reaction centers in polyvinyl alcohol films and in glycerol/buffer glasses. We also examine the dichroism of the absorption changes due to transient states P^+I^- and $P^+Q_A^-$ in films at low temperature.

Materials and Methods

The picosecond transient absorption spectrometer used in these studies has been described previously [11]. Excitation flashes at 600 nm, 30 ps in duration and containing up to 200 μJ, were generated by stimulated Raman scattering from 532-nm pulses in $C_6{}^2H_{12}$. Excitation flashes at 867 nm, 20–25 ps in duration and containing 1 μJ or less, were similarly generated in $C_6{}^2H_{12}$ from 1064-nm pulses. The excitation light was focused to a diameter of 1.5–2 mm at the sample. Photon densities were kept well below the level required to cause the spectral distortions and the 30-ps kinetic component near 800 nm reported previously (and reproduced in our laboratory) when excessively strong excitation is used [2,10]. The picosecond laser was operated at 5 Hz. Making use of two-dimensional vidicon detection, we acquired data over a 150-nm interval on each laser shot.

Reaction centers from *Rps. sphaeroides* (R26) were isolated by standard methods [22]. Polyvinyl alcohol films, which offer the distinct advantage that they do not crack at low temperature as glycerol/buffer glasses often do, were prepared as previously described [20].

Two different films were used, made from different preparations of reaction centers. Film No. 2 was the less concentrated of the two, having $A_{802} \approx 0.25$ (295 K). The quinone content of the reaction centers used to make this film was evaluated at room temperature by comparing the ratio of the fast (≈ 100 ms) and slow (seconds) recovery of the absorbance changes at 425 nm following a 10-ns flash [23]. It was determined that at least 80% of the reaction centers contained only one ubiquinone. This film was cut into eight pieces. Two pieces were stacked together and used to acquire transient spectra and kinetics in the near-infrared. All eight pieces were stacked together and used for measurements between 500 and 750 nm. In picosecond experiments at room temperature a fraction of the reaction centers in the film did not recover in the 200-ms interval between excitation flashes, giving small absorption changes due to P^+Q^- before $t = 0$. (At these negative delays the probe pulse arrives before the pump pulse.) Film No. 1 had $A_{802} = 1.9$ (295 K), and a higher percentage ($\approx 50\%$) of its reaction centers contained two quinones. This film gave a larger signal before zero-time at room temperature in the picosecond apparatus. Single pieces of film No. 1 (optically of better quality than a large stack) were used for spectra and kinetics in the visible (500–750 nm) at low temperature; it was too concentrated for use in the near-infrared. Most of our measurements on films were made at temperatures below 200 K, where electron transfer from Q_A^- to the secondary quinone (Q_B) is blocked [24] and where the time constant of the $P^+Q_A^-$ back-reaction has decreased (from approx. 100 ms at 295 K to approx. 30 ms at 76 K [25–27]). At temperatures below 200 K no absorption changes could be detected before zero-time with either film, indicating that the reaction centers recovered completely between excitation flashes. The two films gave spectra and kinetics that were within experimental error of each other where comparisons could be made. At temperatures above 200 K only film No. 2 was used, in

order to minimize potential artifacts due to the presence of reaction centers in the state $P^+Q_B^-$. At room temperature, film No. 2 gave kinetics and spectra that agreed with those obtained with flowed solutions of reaction centers in buffer.

Low-temperature measurements were performed with an Oxford Instruments liquid-helium flow cryostat system model CF204. Liquid nitrogen was used for measurements at 76 K and above. The cryostat controls to within ± 0.1 K, using a temperature sensor in the heat-exchanger block through which the cryogen flows. To ensure that the sample was also at the desired temperature we equipped the sample compartment with a chromel/gold 0.07 atom% iron thermocouple calibrated with a digital temperature-indicator accurate to ± 0.5 K (Scientific Instruments). This thermocouple was sandwiched along with the film between two glass plates in the sample compartment, or placed within the glycerol/buffer solution. The two temperature indicators read within 1 K of each other throughout the course of an experiment. Samples were always cooled in the dark.

Kinetics were determined by fitting the time dependence of the absorption changes in 2–10-nm intervals at wavelengths where the difference between the initial and final values of ΔA was 0.05 or more. Most of the computer analyses were performed on a Tektronix 4052 computer using Plot 50 statistics software, which included nonlinear least-squares fitting programs based on the Marquardt and Gauss-Newton methods. Other fits were done on a Tektronix 4165 computer as described elsewhere [22].

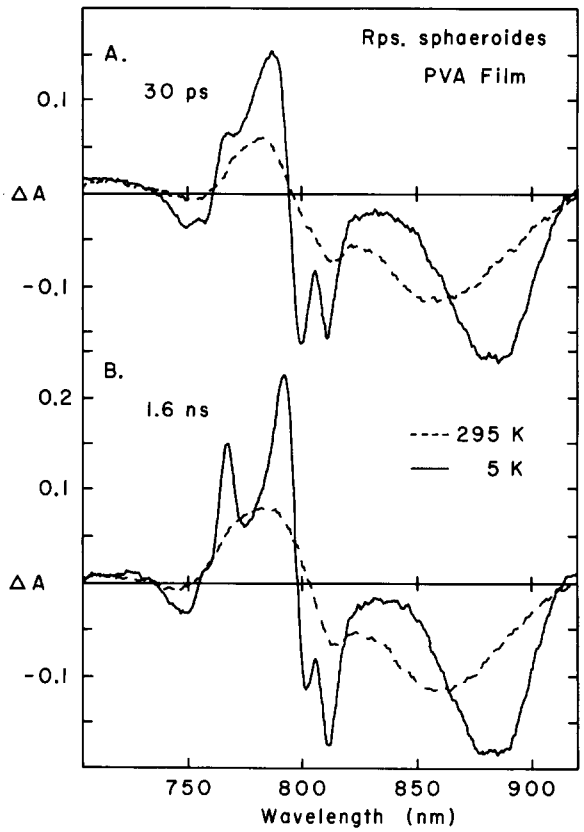

Fig. 1. Near-infrared absorption changes for *Rps. sphaeroides* reaction centers imbedded in a polyvinyl alcohol film at 30 ps (A) and 1.6 ns (B) with respect to the center of a 30-ps 600-nm excitation flash, at 295 K (dashed) and 5 K (solid). All spectra were acquired using the same 2-piece stack of film No. 2. Each spectrum was acquired in two 150-nm slices that agreed within experimental error in the regions of overlap. Each spectrum shown here and in the next figure represents the average of data acquired using approx. 300 excitation flashes and has a maximum error in ΔA of ± 0.005 over the wavelength region shown.

Results

Comparison of transient-state spectra at 295 K and 5 K

Fig. 1 shows the near-infrared difference spectra for the formation of states P^+I^- (A) and $P^+Q_A^-$, hereafter referred to as P^+Q^-, (B) in *Rps. sphaeroides* reaction centers imbedded in a film at 295 K (dashed) and at 5 K (solid). The spectra were recorded at 30 ps and 1.6 ns with respect to the peak of a 30-ps, 600-nm excitation flash. Fig. 2 shows the corresponding difference spectra in the visible region on an expanded ΔA scale for a film having approx. 4-times the absorbance (see Materials and Methods). The spectra of Figs. 1 and 2 overlap between 700 and 750 nm. The absorption changes at 295 K are similar to those observed previously using single-wavelength [2,5,6,9,13] and broad-band [11,28] detection with *Rps. sphaeroides* reaction centers in buffer at room temperature. The difference spectra are much better resolved at 5 K than at 295 K (Figs. 1 and 2). As the temperature is lowered, bleaching in the long-wavelength band of P sharpens and increases

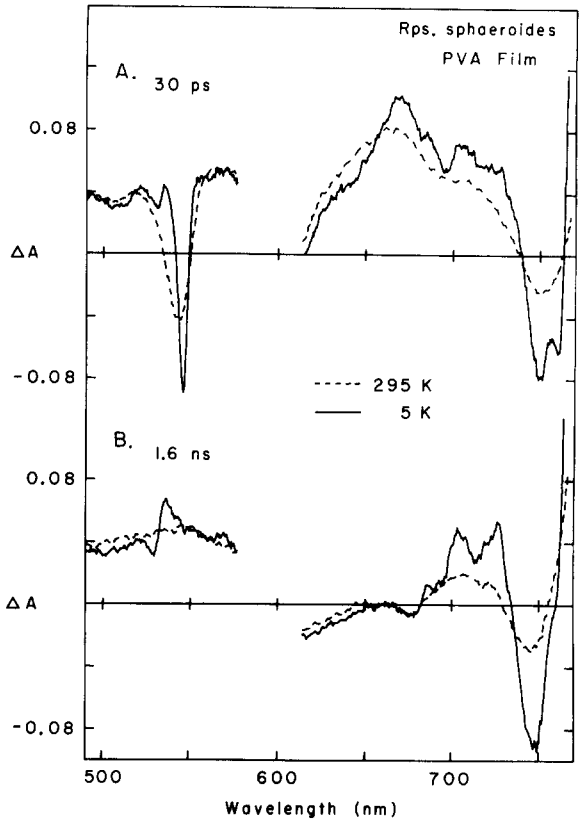

Fig. 2. Absorption changes in the visible region acquired as in Fig. 1, except that the polyvinyl alcohol film (No. 1) had approx. 4-times the absorbance. Other conditions as in Fig. 1.

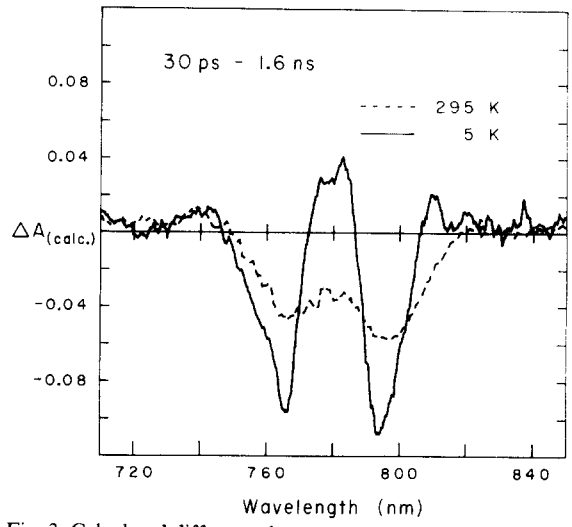

Fig. 3. Calculated difference between the absorption changes at 30 ps and 1.6 ns from Fig. 1 at 295 K (dashed) and 5 K (solid).

in peak amplitude; the peak position shifts from 855 nm at 295 K to 880 nm at 5 K (Fig. 1). These temperature variations correspond to changes in the ground-state absorption spectrum [21]. Similar, but not identical, changes in transient-state and ground-state spectra occur in glycerol/buffer glasses [4,21,29–31]. The absorption changes between 780 and 830 nm are probably attributable mainly to the two BChls not involved in P, and the absorption changes between 720 and 770 nm to the two BPhs. The general sharpening of these spectral features at lower temperature allows a clearer distinction between the two spectral regions. The splitting observed at low temperatures at 800 and 812 nm in the transient spectra is a prominent new feature in the films. (The ground-state absorption spectrum of reaction center films at low temperature exhibits a shoulder at 812 nm on the strong absorption band centered at 802 nm [21].)

Fig. 3 shows the difference between the absorption changes measured in the near-infrared at 30 ps (Fig. 1A) and those at 1.6 ns (Fig 1B) at 5 K and 295 K. It is normally assumed that such difference-difference spectra emphasize the absorption changes caused by reduction of I. The clear separation between the major features centered at 765 and 795 nm is revealed in the 5 K spectrum (solid). Also notable in the low-temperature spectrum is an asymmetry of the negative feature in the shorter-wavelength region attributable to BPh. There appears to be a sharp absorption decrease at 765 nm and broader feature tailing to the blue.

The difference spectra in the visible region include two major bands in which the conversion of P^+I^- (Fig. 2A) to P^+Q^- (Fig. 2B) can be monitored. In the next section we examine the kinetics of this step, as measured by the decay of (1) the bleaching in the 545-nm Q_X absorption band of the BPh and (2) the broad absorption increase near 665 nm due to I^-. Both features are best resolved at low temperature (Fig. 2A). The 530-nm Q_X band of the second BPh is resolved in the low-temperature ground-state spectrum [21,29–31], and appears to be red-shifted in the P^+Q^- spectrum (Fig. 2B) [32]. The difference spectrum for

state P^+Q^- at low temperature shows a double-banded feature between 690 and 730 nm (Fig. 2B). These absorption changes appear to be present in the P^+I^- difference spectrum as well (Fig. 2A), suggesting that they may be due largely to the oxidation of P.

Temperature dependence of the $P^+I^- \rightarrow P^+Q^-$ kinetics detected in the visible region in films

Fig. 4 presents a typical set of kinetic data. Shown here is the decay of the 665-nm absorption band of I^-, produced by excitation with 600-nm flashes at 5 K. The solid curve is a nonlinear least-squares fit to the function $\Delta A = \Delta A_\infty + \Delta A_0 \cdot \exp(-t/\tau)$, where τ is the time constant, ΔA_∞ is the absorption change at the asymptote (long time) and $\Delta A_\infty + \Delta A_0$ is the absorption change at $t = 0$. Only data obtained at delay times of 30 ps and longer were fit. The lifetime determined from the data of Fig. 4 is 94 ± 6 ps.

Fig. 5 shows the temperature dependence of the decay kinetics, as measured in films at 545 nm (circles) or 665 nm (triangles). The left ordinate is the rate constant $k = 1/\tau$ in s^{-1}, and the right ordinate scale shows the decay time τ in picoseconds. The measurements at all wavelengths and

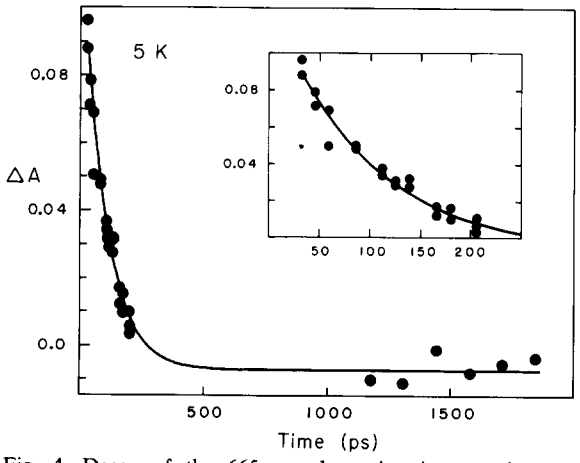

Fig. 4. Decay of the 665-nm absorption increase in *Rps. sphaeroides* film No. 2 at 5 K following excitation with a 30-ps 600-nm flash. The standard deviation in ΔA for these data is ± 0.005. The inset shows the decay portion of the kinetics on an expanded time (picosecond) scale. The solid curve in both the main figure and the inset is a nonlinear least-squares fit to an exponential function (see text), giving a decay time of 94 ± 6 ps.

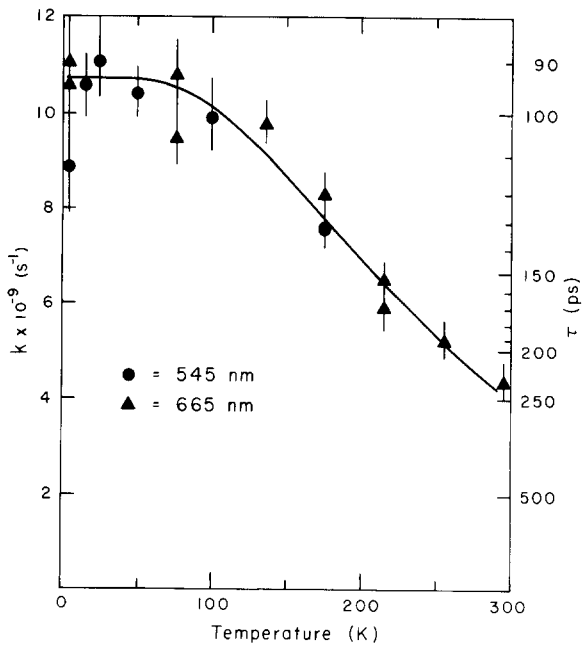

Fig. 5. Temperature dependence of the rate of electron transfer from BPh^- to Q in *Rps. sphaeroides* polyvinyl alcohol films measured at 545 nm (circles) and 665 nm (triangles). Kinetics were measured following excitation with 30-ps 600-nm excitation flashes. The solid curve is a fit to the experimental data using the theory of Kakitani and Kakitani [38] with $\nu_e/c = 250$ cm^{-1}, $\langle \nu_g/c \rangle = 1550$ cm^{-1}, $S = 0.6$, $\Delta G(295\ K) = 4000$ cm^{-1}, $\Delta E_1 = 2400$ cm^{-1}, and $V = 30$ cm^{-1}.

temperatures are described well by first-order kinetics. The error limits for individual lifetime measurements are typically ± 5–10%. The electron-transfer rate constant increases by a factor of approx. 2.3 as the temperature is lowered from 295 K to near 80–100 K, at which point the rate becomes independent of temperature within experimental error. The mean lifetime below 100 K is 97 ± 8 ps. These data for films are summarized in the third and fourth columns of Table I. The time constant of 229 ± 25 ps measured at 665 nm in film No. 2 at 295 K (Table I) agrees well with the time constant of 207 ± 12 ps (average of four measurements at 665 nm in Table I) determined on flowed reaction centers in buffer at 288 K. The solid curve through the experimental data in Fig. 5 is a theoretical fit that will be discussed below.

Detection-wavelength dependence of the observed kinetics

The $P^+I^- \rightarrow P^+Q^-$ decay kinetics measured in films at temperatures below 100 K are the same within experimental error, whether they are measured at 545 nm or in the 665-nm region (Fig. 5

TABLE I

SUMMARY OF DECAY KINETICS IN *RPS. SPHAERODIES* REACTION CENTERS

Data are lifetimes in picoseconds. Data were obtained using 30-ps 600-nm flashes except for (f). For film No. 2, near-infrared measurements employed a 2-stack, whereas those in the visible employed an 8-stack (see Materials and Methods). The temperature of the flowed reaction centers near room temperature was 288 ± 5 K.

Sample	Temp. T (K)	545-nm band [a]	665-nm region [b]	758 nm [c]	765 nm [c]	795-nm region [d]
Film 1	5	113 ± 13	90 ± 7			
Film 2	5		94 ± 6	140 ± 20	104 ± 11	70 ± 10
Film 2	5					76 ± 11 [e]
Film 2	5					74 ± 12 [e,f]
Film 1	15	94 ± 7				
Film 1	25	90 ± 8				
Film 2	50	96 ± 5				
Film 1	76		92 ± 6			
Film 2	76		105 ± 7	134 ± 18	108 ± 12	65 ± 5
Film 2	76					74 ± 8 [e]
Film 2	76					67 ± 10 [e]
Film 1	100	101 ± 8				
Film 1	135		102 ± 5			
Film 1	175	132 ± 7	120 ± 6			
Film 2	175		133 ± 7			
Film 2	215		153 ± 9			
Film 2	215		169 ± 15			
Film 2	255		192 ± 17			
Film 2	295		229 ± 25		218 ± 30 [g]	154 ± 15
Buffer [h]	288	250 ± 17	194 ± 15		241 ± 25	164 ± 12
Buffer [h]	288	251 ± 13	198 ± 15		250 ± 23	160 ± 11
Buffer [i]	288	247 ± 12	219 ± 15		240 ± 25	147 ± 12
Buffer [j]	288	263 ± 13	215 ± 20		266 ± 20	127 ± 10
Buffer averager:		253 ± 10	207 ± 12		249 ± 12	150 ± 17
56% glycerol	76				130 ± 11	92 ± 5
65% glycerol	76				127 ± 9	103 ± 10

[a] Averaged absorption changes between 542 and 547 nm.

[b] Averaged absorption changes between 660 and 670 nm. Time constants determined for the intervals 650–660 nm and 670–680 nm were the same within experimental error.

[c] Lifetime decreased with increasing detection-wavelength between 755 and 770 nm in the films at 5 K and 76 K. At these temperatures the entries are for kinetics measured at 757–759 nm and 764–766 nm. For the 295 K measurement on the film and the 288 K measurements in flowed buffer, the time constant was determined over the range 761–767 nm only, because of the small amplitude of the absorbance changes. For the glycerol/buffer glasses at 76 K no clear systematic variation in kinetics with detection wavelength was observed in the 755–770 nm region, and the entry represents an average of time constants determined across this region.

[d] Average of time constants measured at 3–5-nm intervals between 790 and 800 nm.

[e] Employed 805 nm interference filter between the sample and monochromator to isolate 795 nm region.

[f] Employed very weak 867-nm flashes.

[g] Smaller change in ΔA at 765 nm (0.04) than we normally used for measuring kinetics.

[h] Flowed reacion centers in 10 mM Tris-HCl (pH 8.0)/0.05% Triton X-100.

[i] Same buffer as (h), but different preparation of reaction centers.

[j] Flowed reaction centers in the same buffer as (h), but prepared by P. Maroti and C. Wraight, University of Illinois, Urbana, IL.

and Table I). The time constants measured across the 665-nm band (650–680 nm) are the same within experimental uncertainty at a given temperature. However, the decay kinetics measured in the near-infrared region are, in general, different from those measured in the visible region. These new observations are most readily discussed in conjunction with the difference-difference spectra of Fig. 3. The 765-nm feature (750–770 nm) is normally attributed to BPhs, while the 795-nm feature (785–805 nm) is normally attributed to the BChls. The lifetimes measured at 758 and 765 nm and in the 795-nm region are summarized in the last three columns of Table I.

The lifetimes measured in both the 765- and the 795-nm regions decrease by a factor of approx. 2 when the temperature is lowered from 295 K to 76 K. In each region, the lifetime is the same within experimental error at 76 K and 5 K. This temperature dependence is very similar to that observed in the visible (Fig. 5 and Table I). However, the lifetime within the 795-nm feature is approx. 155 ps at 295 K and approx. 70 ps at both 76 K and 5 K. These decay times are significantly shorter than the values of approx. 230 ps (295 K) and approx. 100 ps (76 and 5 K) determined from the measurements in the visible region or at 765 nm (Table I).

A rapid ($\leqslant$ 30 ps) relaxation near 800 nm [2,10] (near 830 nm in *Rps. viridis* [33]) has been observed previously (and reproduced in our laboratory) when excessively strong excitation flashes are employed. This rapid step is accompanied by dramatic distortions in the transient spectra at delay times less than 30 ps, including an 'extra' bleaching at 800 nm. Such spectral distortions and kinetics were never observed in the present study, in which relatively weak excitation flashes at 600 nm were employed (see Materials and Methods). However, we still considered the possibility that the shorter lifetimes observed in the 795-nm feature could be related to excitation of one of the two BChl molecules not involved in P. This was tested by carrying out two additional measurements. First, we attempted to measure transient spectra and kinetics in reaction centers (in buffer at 295 K) in which P was pre-oxidized with $K_3Fe(CN)_6$. In these reaction centers only a very small bleaching is observed at 795 nm during the 30-ps 600-nm excitation flash, even when the flash

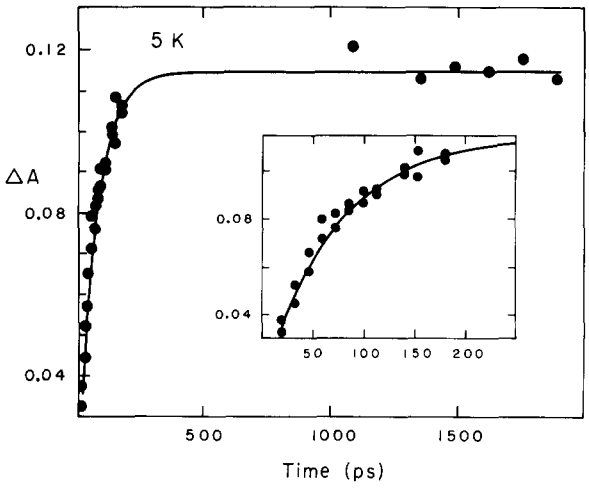

Fig. 6. Growth of the absorption increase at 795 nm (see Figs. 1 and 3) following excitation of *Rps. shpaeroides* polyvinyl alcohol film No. 2 at 5 K with approx. 20-ps 867-nm flashes. The probe pulses were polarized parallel to the excitation pulses. Other conditions as in Fig. 4. The decay time constant is 70 ± 10 ps.

strength is increased 3-fold over that normally used. The bleaching recovers by approx. 50 ps, indicating that the lifetime of the transient is less than 15 ps. Second, we measured kinetics in the 795-nm feature following excitation of reaction centers in a film at 5 K with weak 867-nm flashes. Fig. 6 shows experimental data and computer fit for decay of the absorption changes in the interval 794–796 nm; the decay time is 70 ± 10 ps. The average lifetime for this and adjacent 3-nm intervals is 74 ± 12 ps (Table I). This lifetime is the same within experimental error as those determined from the measurements using the stronger 600-nm flashes.

Some of the measurements in the 795-nm band, including that of Fig. 6, employed an 805-nm interference filter (25-nm bandwidth) in the probe beam between the sample and the detection monochromator. The filter was used to insure that sufficient probe light reached the vidicon in this spectral region without overloading the vidicon in adjacent regions where the ground-state absorption is much lower. As can be seen from Table I, at a given temperature the lifetimes in the 795-nm region are the same within experimental error as those obtained in the absence of the interference filter.

Kinetic determinations in the 765-nm region (Fig. 3) could be made simultaneously with those in the 795-nm region when no interference filter was placed in the probe light. At low temperature we find evidence for a variation in lifetime with wavelength within the 765-nm feature. The lifetimes appear to be longer when measured on the short-wavelength side of the band (for example, at 758 nm) compared to the trough (765 nm) or to the long-wavelength side. (Compare entries in the fifth and sixth columns of Table I at 5 and 76 K.)

The decay kinetics in the near-infrared region listed in Table I were obtained by fitting the experimental points in the same manner as was done for the kinetics in the visible region. Good fits to single-exponential decay functions were obtained in all cases. We also attempted to deconvolute the 795-nm kinetics from an instrument function, to insure that the approx. 70 ps lifetime measured at low temperature was not skewed due to convolution of the decay with the 30-ps pump and probe pulses. These deconvolution fits were done using the 76 K data. To obtain an instrument response function, we accurately measured the apparent rise-time of the absorption changes at 785 nm at 76 K. Because 785 nm is an isosbestic wavelength between the P^+I^- and P^+Q^- difference spectra at 76 K (and also at 5 K, Fig. 3), the apparent growth of the absorption change at this wavelength is not perturbed by convolution with a decay. (The absorption changes over the entire 750–830 nm region, however, all appear to lag behind bleaching of the 865-nm band of P by approx. 6 ps at room temperature, as discussed elsewhere [4]). The 785-nm rise-time data were differentiated to get an instrument function, which was then convoluted with an exponential plus a constant. The resultant function was used to fit the entire rise and decay kinetics at other wavelengths in the 750–800 nm region. This second fitting procedure gave (to within 10%) the same approx. 70 ps decay time in the 795-nm region as was determined from the single-exponential fits. In the measurement where kinetics in the 765-nm region were determined simultaneously, the deconvolution procedure also indicated that the lifetime decreases from approx. 135 ps at 758 nm to approx. 105 ps at 765 nm.

Thus, the difference in kinetics in the 795- and 765-nm regions reported in Table I and the differences from the kinetics determined in the 545- and 665-nm regions are not due to artifacts caused by detection electronics or optics, pump wavelength, pump intensity, or pulse convolution.

A dramatic variation in the observed decay kinetics with detection wavelength also was seen with flowed *Rps. sphaeroides* reaction centers in buffer at 288 K. Table I summarizes four sets of kinetic data obtained using 600-nm excitation flashes for reaction center preparations from two laboratories. The average lifetime of 253 ± 10 ps at 545 nm is the same within experimental error as that of 249 ± 12 ps observed near 765 nm. (Because the absorption changes at room temperature in the 755–770-nm region are small (Figs. 1 and 3), we could only measure kinetics in the interval ≈ 761 to ≈ 768 nm, at the peak of the 765-nm feature.) The lifetime in these two regions is somewhat longer than the average value of 207 ± 12 ps measured across the 665-nm absorption increase. A substantially shorter average time constant of 150 ± 17 ps was measured in the 795-nm region (Table I). We note also that the transient spectra in the 795-nm region are very sensitive to the medium (environment). The splitting into two troughs at 800 and 812 nm seen in films (Fig. 1) is not observed at low temperature with reaction centers in 65% glycerol, and is just barely resolvable with 56% glycerol [21]. Listed last in Table I are the results from two kinetic measurements in glycerol/buffer glasses at 76 K.

In summary, variations in decay kinetics with detection wavelength have been observed for *Rps. sphaeroides* reaction centers at room temperature, 76 K and 5 K. However, the temperature dependence of the kinetics is similar in all of the absorption bands.

Discussion

Temperature-dependence of the $P^+I^- \rightarrow P^+Q^-$ rate

Two previous studies on the temperature dependence of the $P^+I^- \rightarrow P^+Q^-$ electron transfer rate in *Rps. shpaeroides* reaction centers have been carried out. Peters et al. [19] measured the decay kinetics with reaction centers in glycerol/buffer solution. Measurements at 640 nm were made at

295 K, 58 K and 5 K, and measurements at 545 nm were made at 295 K and 5 K. Peters et al. reported lifetimes of approx. 150 ps from all of these measurements, and concluded that the rate of electron transfer was independent of temperature from 295 K to 5 K. Schenck et al. [20] measured decay times with *Rps. sphaeroides* reaction centers in films similar to those employed in the present study. Kinetics were monitored at 650 nm for most of the measurements. The decay time constant decreased from 220 ps at 295 K to 105 ps near 50 K. The increase in rate by a factor of 2.1 over this temperature range is in good agreement with the factor of approx. 2.3 (229 ps to 97 ps) found in the present study (Table I). However, Schenck et al. measured a time constant of 65 ps at 25 K and 190 ps at 8 K, with a value of 100 ps at the intermediate temperature of 15 K. The sharp rise in rate at 25 K and sharp decrease below 10 K reported by Schenck et al. was not reproduced in the present study. Because of the increased repetition rate and the two-dimensional detection technique, the quality of the spectral and kinetic data is much higher in the present measurements than in the earlier studies. Thus, we view the results shown in Fig. 5 and summarized in Table I as giving the correct temperature dependence of the rate of electron transfer from I^- to Q in *Rps. sphaeroides* reaction centers.

Theories for photosynthetic electron transfer normally begin with the premise that the electron transfer is nonadiabatic [34–41]. This means that the electronic coupling between reactants and products is small, because of poor orbital overlap between the electron donor and acceptor. This view is based on the idea that the protein holds the electron carriers in fixed positions and orientations that may not give substantial orbital overlap. Expressions for the rate of electron transfer in the nonadiabatic formulation are derived by using first-order perturbation theory, which leads to a Fermi-golden-rule equation for the rate: $W = 4\pi^2 h^{-1} V^2 F$, where h is Planck's constant, V is the electronic (tunneling) matrix element between the donor and acceptor, and F is the thermally weighted Franck-Condon (vibrational overlap) factor.

We have considered two possible interpretations for the temperature dependence of the rate of electron transfer from I^- to Q. First, the effects of temperature on the kinetics could be rationalized on the basis of changes in conformation of the protein [42]. The increase in electron transfer rate could be accounted for if I^- and Q move closer together or into an increasingly more favorable geometry as the temperature is reduced. The electronic factor (V) is thought to decrease exponentially with distance: $V = V_0 \cdot \exp(-\beta R)$, with $\beta \approx 10\ \text{nm}^{-1}$ [35,43]. The increase in rate by a factor of approx. 2.3 would mean that the distance between I^- and Q decreases by about 0.1 nm as the temperature is lowered from 295 to 100 K. This interpretation requires that the conformation remain constant below 100 K, where the rate is independent of temperature.

An alternative interpretation is that V is independent of temperature, and that the variation of the electron transfer rate with temperature is contained in the thermally weighted Franck-Condon factor [34–38]. This interpretation is attractive, because it suggests a possible connection between the temperature dependence of the electron-transfer kinetics and the temperature dependence of the spectral widths of certain bands in the reaction center's absorption spectrum [39,44]. The bandwidths show variations with temperature comparable to the changes in the electron-transfer rate [21].

Jortner obtained an expression for the rate (Eqn. 3a of Ref. 34) in which the Franck-Condon factor depends on both high-frequency quantum (pigment) modes and low-frequency solvent (medium) modes. In applying this theory to photosynthetic electron transfer, Jortner proposed that high-frequency quantum modes having an average value of $\langle \nu_q \rangle / c \approx 400\ \text{cm}^{-1}$ make the dominant contribution to the Franck-Condon factor (c is the speed of light) [34,35]. Jortner showed that the rate of electron transfer will be maximal when the overall energy change in the reaction ($\Delta E = P \cdot h\langle \nu_q \rangle$) is equal to the vibrational reorganization energy, $S_q \cdot h\langle \nu_q \rangle$. P is the reduced energy gap and S_q is the dimensionless coupling strength, a measure of the configurational changes (changes in bond lengths and bond angles) accompanying electron transfer. (In the convention used by Jortner, and followed below, ΔE is positive for a reaction that is exothermic. The same convention

will be used for the free energy change, ΔG.) The maximal rate condition $P = S_q$ is equivalent to that of $\Delta G = \lambda$ in the classical theory of Marcus [45], and corresponds to the situation where the nuclear potential surface for the product state crosses the minimum in the potential surface for the reactant state; the reaction is 'activationless' or barrierless [35].

An interesting aspect of an activationless electron-transfer reaction is that the rate is expected to show a non-Arrhenius or 'negative-activation' behavior at high temperature and to be independent of temperature below a critical temperature defined by the 'characteristic' frequencies in the problem. At low temperature ($kT \ll h\nu$) only the zero-point vibrational levels will be populated. The rate will be maximal for a given electronic factor V, since the vibrational overlap (Franck-Condon factor) will be optimum. The rate will decrease as the temperature is raised, since higher vibrational levels of the reactants will be thermally populated. These higher vibrational states have poorer overlap with the product vibrational states.

The general qualitative predictions of the theory for an activationless reaction are reproduced in our data for the $P^+I^- \rightarrow P^+Q^-$ reaction (Fig. 5 and Table I). We therefore attempted to fit our data to Jortner's expression in which only one (average) molecular mode contributes. The observed critical temperature of approx. 100 K fixes $\langle \nu_q \rangle / c \approx 300$ cm^{-1}. However, Jortner's expression predicts an increase in rate of at most a factor of approx. 1.2 as the temperature is lowered from 295 K to 100 K, as compared to the measured factor of approx. 2.3.

Sarai [36,37] considered a more general form of Jortner's theory in which the Franck-Condon factor includes explicit contributions from an arbitrary number of vibrational modes. The inclusion of the low-frequency modes can cause a dramatic temperature dependence of the rate. Since the rate of $P^+I^- \rightarrow P^+Q^-$ reaction is independent of temperature below approx. 100 K within our experimental error (Fig. 5), vibrational modes having energies much less than approx. 300 cm^{-1} cannot be used in Sarai's expression for the Franck-Condor factor. If they are included, such low-energy modes make the predicted rate change with temperature below 100 K. Therefore, we attempted to fit our data by including one 300 cm^{-1} mode plus one higher-energy quantum mode (500–2500 cm^{-1}). Then the predicted maximum increase in rate as the temperature was varied from 295 K to 100 K was a factor of approx. 1.2, as in Jortner's single-mode theory. This is expected, since the higher-energy mode will not be significantly populated even at room temperature.

Both Jortner [34,35] and Sarai [36,37] assumed that the frequencies of the vibrational modes do not change in going from reactants to products. Holding the vibrational frequencies constant means that the reactants and products have the same density of vibrational states, so that there is no change in entropy in the electron-transfer reaction [38,39]. The potential energy surfaces for reactants and products have the same shapes, and are simply displaced vertically from one another by the energy gap and horizontally by an amount related to the electron-vibration coupling parameter(s) S. The reduced energy gap P thus is independent of temperature, and the temperature dependence of the rate enters only as the thermal population of the modes $h\langle \nu_q \rangle$.

Kakitani and Kakitani [38] recently developed a theory in which vibrational frequency changes as well as displacements are allowed. This means that the reactants and products can have different densities of vibrational states and that their potential energy surfaces do not have the same shape. The electron-transfer reaction thus can involve a change in entropy. These authors derive an expression (Eqn. 5 of Ref. 38) identical to Jortner's, except that ΔE is replaced by the free energy change ΔG, and the entropy change makes ΔG a function of temperature. Kakitani and Kakitani also argue that molecular vibrations having $\langle \nu_q \rangle / c =$ 1000–1600 cm^{-1} are likely to be the most strongly coupled to electron transfer involving porphyrins because they should exhibit the greatest configurational changes (displacements). This view is based on the fact that modes in this energy range, involving in-plane skeletal vibrations of the atoms in the conjugated π-system, show strong enhancements in the resonance Raman spectra of porphyrins, BChl, BPh and their oxidation products [46–49] and are responsible for intensity borrowing (B $\rightarrow$ Q) as well as the vibrational progressions (Q(0, 0), Q(1, 0), etc.) in the electronic absorption spectra of these molecules [50].

The high-frequency skeletal modes have $h\langle\nu_q\rangle \gg kT$ ($T \leqslant 300$ K), and in this limit the rate expression simplifies to [38]:

$$k = (2\pi/h)\left(V^2/h\langle\nu_q\rangle\right)\cdot\exp(-S)\left(S^P/\Gamma(P+1)\right) \qquad (1)$$

where S is the effective electron-vibration coupling strength for the high-frequency modes, $\Gamma(P+1)$ is the gamma function, and $P = \Delta G/h\langle\nu_q\rangle$ is the reduced free-energy gap. Besides the mathematical simplifications giving rise to Eqn. 1, the condition $h\langle\nu_q\rangle \gg kT$ has an important consequence for the calculation of the Franck-Condon factor. In the theory of Kakitani and Kakitani [38] the high-frequency vibrational modes $h\langle\nu_q\rangle$ that involve the largest displacements, and define the reaction coordinate, are not excited significantly above their zero-point levels, even at 300 K. Therefore, the temperature dependence of the electron-transfer rate is not determined by the thermal population of these modes, as it is in theories of Jortner and Sarai [34–37]. The condition for an activationless reaction has become $h\langle\nu_q\rangle \gg kT$, and is much less dependent on the relationship between P and S [38].

The temperature dependence of the electron-transfer rate in the theory of Kakitani and Kakitani is determined by the thermal population of the vibrational modes that experience changes in frequency. These modes could not be assigned explicitly and were characterized by an average frequency ν_e. The effective thermal weighting of these modes is

$$n_e = \left(\exp\left(h\nu_e/kT\right)-1\right)^{-1} \qquad (2a)$$

The total free energy change thus becomes

$$\Delta G = \Delta E + Nh\Delta\nu_e/2 + Nh\Delta\nu_e n_e$$

$$= \Delta E + \Delta E_1(1/2 + n_e) \qquad (2b)$$

where $\Delta\nu_e$ is an average change in frequency, N is the total number of modes and $\Delta E_1 = Nh\Delta\nu_e$. The term $Nh\Delta\nu_e/2$ represents the shift in zero-point energy, and the term $Nh\Delta\nu_e n_e$ is the entropic contribution to the free energy, due to the change in vibrational frequencies between reactants and products. If N is large, ΔE_1 can be substantial even though $\Delta\nu_e$ is relatively small. The temperature dependence thus is contained in the reduced energy gap parameter $P = \Delta G/h\langle\nu_q\rangle$ via the temperature dependence of ΔG in Eqns. 2a and 2b. The critical temperature separating the regions of temperature dependence and temperature independence is defined by the characteristic energy $h\nu_e$ (Eqn. 2a). Fitting the data of Fig. 5 requires that $\nu_e/c = 250$–300 cm^{-1}. Although this value is necessarily similar to that required by Jortner and Sarai, the physical significance of the modes $h\nu_e$ is much different from that of the modes $h\langle\nu_q\rangle$, as discussed above and further below.

The solid curve in Fig. 5 is a computer fit using Eqns. 1 and 2 above with $\nu_e/c = 250$ cm^{-1}. Combinations of the other adjustable parameters in the following ranges give similar fits: $\langle\nu_q\rangle/c =$ 1000–1600 cm^{-1}, $S = 0.5$–1.0, $\Delta G(295\ \text{K}) =$ 3000–5000 cm^{-1}, $\Delta E_1 =$ 2000–3000 cm^{-1}, and $V =$ 15–30 cm^{-1}.

As discussed above, a value of $\langle\nu_q\rangle/c =$ 1000–1600 cm^{-1} is likely to be appropriate for electron transfer from I^- to Q. A value of $S \approx 1$ associated with the modes $h\langle\nu_q\rangle$ appears to be physically reasonable for electron transfer involving porphyrins (BPh and BChl) and quinones (Q), considering the typical changes in bond lengths and angles observed upon excitation or oxidation/reduction [36,38,46]. Warshel [40] has come to a similar conclusion. He used $\langle\nu_q\rangle/c =$ 1400 cm^{-1} and $S = 0.7$ in discussing the kinetics of the primary reactions.

It is assumed that the energy change ΔE is independent of temperature [38]. We fix ΔE using Eqn. 2 by using a room-temperature free-energy change $\Delta G(295\ \text{K})$ of 4000 cm^{-1}, a value that appears to be appropriate for the $P^+I^- \rightarrow P^+Q^-$ reaction on the basis of available data [17,51,52]. A ΔE_1 of 2000–3000 cm^{-1} appears also to be resonable, considering the large number of vibrational modes available in the porphyrin, the quinone and the protein [38]. The positive value of ΔE_1 required to give the decrease in rate with increasing temperature means that the average vibrational frequency ν_e decreases as the electron is transferred from I^- to Q. A decrease in vibrational level spacing means that the density of vibrational states is higher in the products than in the reactants. This corresponds to an entropy increase as a result of the electron transfer. The

theoretical fit suggests that the absolute magnitude of the free-energy difference (ΔG) between P^+I^- and P^+Q^- decreases by 500–1000 cm^{-1} as the temperature is lowered from 295 to 100 K.

The electronic parameter V scales the entire curve to give the proper rates. Using the simplified formulation given above that V decreases exponentially with distance, and using $V_0 = 10^5\ cm^{-1}$ [35], we find that to fit our data requires $V = 15$–$30\ cm^{-1}$ and $R = 0.8$–0.9 nm. This edge-to-edge distance between BPh and Q is close to that found in the crystal structure of the *Rps. viridis* reaction center [53]. However, the simple exponential relationship of V to distance was derived assuming a specific electron-tunneling barrier height (V_0) and also contains no orientation factor [34,35]. Therefore, the distance obtained using this relationship may not be highly accurate.

Except for V, the values of the parameters used here to fit the temperature dependence of the $P^+I^- \rightarrow P^+Q^-$ reaction are similar to those used by Kakitani and Kakitani [38] to fit the data for the $P^+Q^- \rightarrow PQ$ recombination reaction in *Rps. sphaeroides*. The V factor differs because of the difference in the time scales (and distances) for the two processes. The alternative interpretation that the temperature dependence of the kinetics is contained solely in the electronic factor V requires that the distances between P^+ and Q^- and between I^- and Q both decrease as the temperature is reduced from 295 K to approx. 100 K and remain constant at lower temperatures.

Finally, we inquire as to the nature of the low-energy modes that change frequency upon electron transfer. These modes govern the entropy change and the temperature dependence of electron transfer in the theory of Kakitani and Kakitani [38]. There must be an important class having an average energy $\nu_e/c \approx 250$–$300\ cm^{-1}$ in order to obtain the proper critical temperature of approx. 100 K for the $P^+I^- \rightarrow P^+Q^-$ step (Fig. 5). Hydrational modes are in the proper energy range [54]. However, Kakitani and Kakitani point out that the protein may exclude solvent molecules from the pigment environment. Porphyrins have a number of out-of-plane deformation modes at energy $< 1000\ cm^{-1}$. The 400–600 cm^{-1} modes that involve mainly folds, swivels, tilts and translations of the pyrrole groups describe local motions of the same structural elements as the high-energy modes that are strongly coupled to the electron transfer [46,47,50]. The protein undoubtedly has a very large number of low-energy modes, some of which may change in frequency when an electron is transferred from I^- to Q. However, assigning ν_e to one particular type of vibration may be improper, since a large number of vibrational modes may change frequency upon electron transfer and they may not contribute equally to the average (Eqn. 2).

Detection-wavelength dependence of the observed kinetics

The results presented here, taken together with a further analysis of the temperature dependence and dichroism of the spectra [21], suggest that the rate of the process $P^+I^- \rightarrow P^+Q^-$ is best measured via the decay of the broad absorption increase near 665 nm in the P^+I^- spectrum (Fig. 2). This band is relatively insensitive to temperature and appears to have only one underlying component. The time constants measured across the 665-nm band (650–680 nm) are the same within experimental uncertainty at a given temperature. The band is well-separated from ground-state absorptions, which are sensitive to temperature, electrochromic, excitonic and other effects. The broad 665-nm absorption increase in the P^+I^- spectrum is consistent with the formation of the anion radical of either BPh or BChl [55–57].

As discussed in Results (Table I), the decay times measured at low temperature in the 665-nm band appear to be the same as the kinetics of the absorption changes at 545 and 765 nm normally attributed to a BPh. For example, between 5 K and 76 K relaxation of the 665-nm absorption increase (95 ± 9 ps) is the same as decay of the bleaching at 545-nm (98 ± 12 ps) (average of values in films in Table I). These times are the same within experimental error as the relaxation of 104–108 ± 12 ps at 5 K and 76 K measured in the sharp 765-nm trough in the low-temperature difference-difference spectrum (Fig. 3). The agreement is particularly good, considering that the 765-nm kinetics could be skewed by the longer-lived component (134–140 ± 20 ps) found at low temperature at 758 nm. The slower decay kinetics measured at 758 nm could reflect an additional relaxation involving the Q_Y band of the second

BPh. (A component of the ground-state absorption that could be the Q_Y band of the second BPh can be partially resolved at approx. 753 nm in derivative spectra of reaction centers in films at low temperature [21]). Such a longer-lived component apparently does not contribute (within our resolution) to the kinetics measured at 545 nm at 5 K or 76 K; the Q_X bands of the two BPhs are well-separated at low temperature, both in the ground-state and the transient-state (Fig. 2) spectra. Therefore, the BPh that receives an electron from P* appears to have its Q_X and Q_Y bands at 545 and 765 nm respectively at low temperature, and evidently forms the anion radical (BPh^-) that gives rise to the 665-nm band in P^+I^- (P^+BPh^-). Picosecond photodichroism measurements at low temperatures show that the 665-nm band has the proper polarization for BPh^- [21].

At higher temperatures there appears to be substantial overlap of the absorption bands (and absorption changes) in both the Q_X and the Q_Y regions of the BPhs [21]. The measurements on the flowed reaction centers at room temperature gave an average time constant of approx. 250 ps at both 765 and 545 nm (Table I). The average time constant across the 665-nm feature is 207 ps, which may, again, reflect the actual rate of electron transfer from I^- (BPh^-) to Q. These observations suggest that an additional slower process contributes to the observed kinetics in the regions of BPh ground-state absorption. This process could be associated with the shorter-wavelength BPh. The slower component of the kinetics in the 750–770 and 530–550 nm regions could reflect a relaxation involving the short-wavelength BPh, following electron transfer. The protein may have to readjust to the new charge distribution on the pigments. A resultant change in local conformation and a repositioning of charged or polar groups on the protein with respect to the pigments could result in shifts in the ground-state (and transient-state) bands of the BPhs and BChls. This model gives a mechanism by which spectral shifts could be observed on pigments that may be spatially far removed from those involved in the electron transfer.

At all temperatures, the decay times measured in the 795-nm region (Fig. 3) are significantly shorter than the time constants measured in the 545-nm, 765-nm and 665-nm regions (Table I). The absorption decrease near 795 nm in the difference-difference spectrum of Fig. 3 (and the absorption decrease seen at this wavelength when I is trapped in the state I^- [13–16]) is usually ascribed to BChl(s) that are involved in some manner with the BPh in I. However, the 795-nm kinetics do not appear to be due to decay of the anion radical $BChl^-$. The results presented here and in a subsequent article [21] favor the view that I^- is largely, if not exclusively, BPh^- since the 665-nm absorption band of P^+I^- (Fig. 2A) appears to be due to BPh^-. The 795-nm kinetics do not appear to be due to exciting the reaction centers with an excessive number of photons, or to an excited state of one of the BChls, as discussed in Results. It seems likely that the absorption change at 795 nm is due predominantly to a change in the interactions of at least one of the neighboring BChls with P, with the BPh that undergoes reduction, or with the protein. The kinetics measured near 795-nm thus could reflect movement of the BChl(s) or readjustment of the protein, following the initial formation of P^+I^-. The initial photooxidation of P may affect the BChls relatively strongly, because they are only 1.1–1.3 nm away (center-to-center), at least in *Rps. viridis* [53]. Excitonic interactions between the BChl(s) and P or BPh would be disrupted. The 795-nm region might be expected to show dramatic absorption changes if some of the absorption near 800 nm in the ground-state spectrum results from such interactions.

One argument against this interpretation of the 795-nm kinetics is the observation that a rapidly decaying component is not observed in this region in reaction centers in which Q is reduced with $Na_2S_2O_4$ prior to excitation (C. Kirmaier, D. Holten and W.W. Parson, unpublished results). However, the prior reduction of Q could cause a conformation change that diminishes the reorganization necessary following the formation of P^+I^-. The reduction of Q is known to have an effect on the BPhs and BChls (and/or the protein), as evidenced by a red-shift of the BPh Q_Y bands and a small blue-shift of the Q_Y bands of the BChls [32]. It has been suggested recently that the formation of P^+Q^- causes a conformation change in the reaction center [58].

We have considered alternative interpretations of the detection-wavelength dependence of the kinetics. One possibility is that the reaction centers may be heterogeneous in some way. However, it would be expected that the kinetics measured in the 665-nm band would be nonexponential and would not correlate solely with the decay of bleachings in the 545- and 765-nm bands of the long-wavelength BPh at low temperature. There also could be at low but finite probability for slower electron transfer through the shorter-wavelength BPh. However, this process might be expected to give a more distinct bleaching near 530 nm than was observed in the low-temperature P^+I^- spectrum, and again probably should affect the kinetics in the 665-nm band of BPh^-. It is also difficult to explain the faster kinetics observed in the 795-nm region of the BChls on the basis of a slow secondary path for electron transfer.

Despite the variation of the kinetics with detection wavelength, the temperature dependence of the kinetics in all spectral regions appears to be similar; the rate increases by a factor of about 2 as the temperature is lowered from 295 K to approx. 100 K, with little or no change between approx. 100 K and 5 K. This observation suggests that the nuclear motions that are important for electron transfer may also play a role in the additional relaxations that we have observed. It is surprising that nuclear relaxations of the pigments and protein that may follow electron transfer might have a non-Arrhenius temperature dependence similar to that of the electron-transfer step itself. Two types of vibrational modes appear to contribute to electron transfer, as discussed above. High-frequency (1000–1600 cm^{-1}) modes are probably the most strongly coupled to electron transfer and undergo the largest displacements. Lower-frequency modes having an average energy of about 300 cm^{-1} may be less strongly coupled to electron transfer, but govern the temperature dependence of the rate. Our observations suggest that either the putative nuclear relaxations involving the BChl(s), the short-wavelength BPh, and/or the protein involve a similar interplay of two types of vibrational modes, or that the relaxations occur most favorably from zero-point vibrational states of modes that have an average energy of the order of 300 cm^{-1}. The temperature dependence of the kinetics of the rebinding of CO to hemoglobin and myoglobin was analyzed recently in terms of two types of vibrational modes [59]. However, the temperature dependence of the kinetics is not the same as observed here for the reaction-center photochemistry, so that the detailed analysis of the two systems is different.

Finally, we note that the temperature dependence of the kinetics is similar to that of the spectral widths of certain bands in the ground-state and transient-state spectra, notably the long-wavelength band of P. Both electron transfer and electronic excitation involve movement of electrons in the π-systems of the bacteriochlorin macrocycles [38,39,44]. High-frequency (1000–1600 cm^{-1}) skeletal modes contribute significantly to the vibrational progressions $Q_{X,Y}(0, 0)$, $Q_{X,Y}(1, 0)$, etc., as noted above [50]. However, the temperature-dependence of the spectra [21] suggests that low-frequency (250–300 cm^{-1}) vibrations may contribute more substantially to the spectral bandwidths.

In summary, we interpret the kinetics associated with the 665-nm band of BPh^- and the 545- and 765-nm bands of BPh as reflecting electron transfer from the long-wavelength BPh^- to Q. Although several questions remain unanswered, we presently view the kinetics of the absorption changes in the 795-nm region of the BChls and in the 530- and 755-nm regions of the short-wavelength BPh as most likely reflecting nuclear relaxations. These pigments could be affected directly by oxidation or reduction of nearby electron carriers or indirectly by readjustment of the protein and its charged groups in response to the new charge distribution on the electron carriers. If this interpretation is correct, it could mean that the primary electron-transfer steps do not involve thermally equilibrated reactant states of the pigments and the protein. This would tend to invalidate an underlying premise upon which most current theories of electron transfer are based [35], including those discussed in this article. Thus, a more complete understanding of the nuclear motions associated with electron transfer in the reaction center may provide new insights into the molecular mechanism of the primary charge separation process.

Acknowledgment

This work was supported by grants PCM-8302477 (D.H.) and PCM-8312371 (W.W.P.) from the National Science Foundation. We thank Drs. Dabney Dixon, Ronald Lovett and Don DeVault for helpful discussions, and Paul Linnemeyer for preparation of reaction centers.

References

1 Parson, W.W. and Ke, B. (1982) in Photosynthesis: Energy Conversion by Plants and Bacteria (Govindjee, ed.), pp. 331–385, Academic Press, New York.
2 Holten, D., Hoganson, C., Windsor, M.W., Schenck, C.C., Parson, W.W., Migus, A., Fork, R.L. and Shank, C.V. (1980) Biochim. Biophys. Acta 592, 461–477.
3 Shuvalov, V.A. and Klevanik, A.V. (1983) FEBS Lett. 160, 51–55.
4 Kirmaier, C., Holten, D. and Parson, W.W. (1985) FEBS Lett. 185, 76–82.
5 Rockley, M.G., Windsor, M.W., Cogdell, R.J. and Parson, W.W. (1975) Proc. Natl. Acad. Sci. USA 72, 2251–2255.
6 Kaufmann, K.J., Dutton, P.L., Netzel, T.A., Leigh, J.S. and Rentzepis, P.M. (1975) Science 188, 1301–1304.
7 Dutton, P.L., Kaufmann, K.J., Chance B. and Rentzepis, P.M. (1975) FEBS Lett. 60, 275–280.
8 Kaufmann, K.J., Petty, K.M., Dutton, P.L. and Rentzepis, P.M. (1976) Biochem. Biophys. Res. Commun. 70, 839–845.
9 Shuvalov, V.A., Klevanik, A.V., Sharkov, A.V., Matveetz, Y.A. and Kryukov, P.G. (1978) FEBS Lett. 91, 135–139.
10 Akhmanov, S.A., Borisov, A.Y., Danielius, R.V., Gadonas, R.A., Kazlowski, V.S., Piskarkas, A.S. and Shuvalov, V.A. (1980) FEBS Lett. 114, 149–152.
11 Kirmaier, C., Holten, D. and Parson, W.W. (1983) Biochim. Biophys. Acta 725, 190–202.
12 Moscowitz, E. and Malley, M.M. (1978) Photochem. Photobiol. 27, 55–59.
13 Schenck, C.C., Parson, W.W., Holten, D. and Windsor, M.W. (1981) Biochim. Biophys. Acta 635, 383–392.
14 Tiede, D.M., Prince, R.C. and Dutton, P.L. (1976) Biochim. Biophys. Acta 449, 447–469.
15 Shuvalov, V.A. and Klimov, V.V. (1976) Biochim. Biophys. Acta 440, 587–599.
16 Okamura, M.Y., Isaacson, R.A. and Feher, G. (1979) Biochim. Biophys. Acta 546, 397–417.
17 Shuvalov, V.A. and Parson, W.W. (1980) Proc. Natl. Acad. Sci. USA 78, 957–961.
18 Pellin, M.J., Wraight, C.A. and Kaufmann, K.J. (1978) Biophys. J. 24, 362–369.
19 Peters, K.S., Avouris, P. and Rentzepis, P.M. (1978) Biophys. J. 23, 207–217.
20 Schenck, C.C., Parson, W.W., Holten, D., Windsor, M.W. and Sarai, A. (1981) Biophys. J. 36, 479–489.
21 Kirmaier, C., Holten, D. and Parson, W.W. (1985) Biochim. Biophys. Acta 810, 49–61.
22 Schenck, C.C, Blankenship, R.E. and Parson, W.W. (1982) Biochim. Biophys. Acta 680, 44–59.
23 Blankenship, R.E. and Parson, W.W. (1979) Biochim. Biophys. Acta 545, 429–444.
24 Parson, W.W. (1969) Biochim. Biophys. Acta 189, 384–396.
25 Parson, W.W. (1967) Biochim. Biophys. Acta 131, 154–172.
26 McElroy, J.D., Mauzerall, D.C. and Feher, G. (1974) Biochim. Biophys. Acta 333, 261–277.
27 Hsi, E.S.P. and Bolton, J.B. (1974) Biochim. Biophys. Acta 347, 126–153.
28 Kirmaier, C., Holten, D., Feick, R. and Blankenship, R.E. (1983) FEBS Lett. 158, 73–78.
29 Clayton, R.K. and Yau, H.F. (1972) Biophys. J. 12, 867–881.
30 Clayton, R.K. and Yamamoto, T. (1976) Photochem. Photobiol. 24, 67–70.
31 Vermeglio, A., Breton, J., Paillotin, G. and Cogdell, R. (1978) Biochim. Biophys. Acta 501, 514–530.
32 Vermeglio, A. and Clayton, R.K. (1977) Biochim. Biophys. Acta 461, 159–165.
33 Holten, D., Windsor, M.W., Parson, W.W. and Thornber, J.P. (1978) Biochim. Biophys. Acta 501, 112–126.
34 Jortner, J. (1976) J. Chem. Phys. 64, 4860–4867.
35 Jortner, J. (1980) J. Am. Chem. Soc. 102, 6676–6686.
36 Sarai, A. (1979) Chem. Phys. Lett. 63, 360–366.
37 Sarai, A. (1980) Biochim. Biophys. Acta 589, 71–83.
38 Kakitani, T. and Kakitani, H. (1981) Biochim. Biophys. Acta 635, 498–514.
39 Hopfield, J.J. (1974) Proc. Natl. Acad. Sci. USA 71, 3640–3644.
40 Warshel, A. (1980) Proc. Natl. Acad. Sci. USA 77, 3105–3109.
41 Blankenship, R.E. and Parson, W.W. (1979) in Photosynthesis in Relation to Model Systems (Barber, J., ed.), pp. 71–114, Elsevier, Amsterdam.
42 Hales, B.J. (1976) Biophys. J. 16, 471–480.
43 Beitz, J.V. and Miller, J.R. (1979) J. Chem. Phys. 71, 4579–4595.
44 Mar, T., Vadeboncoeur, C. and Gingras, G. (1983) Biochim. Biophys. Acta 724, 317–322.
45 Marcus, R.A. (1964) Annu. Rev. Phys. Chem. 15, 155–196.
46 Felton, R.H. (1978) in The Porphyrins (Dolphin, D., ed.), Vol. V, Ch. 3, Academic Press, New York.
47 Spiro, T. (1983) in Iron Porphyrins (Lever, A.B.P. and Gray, H.B., eds.), Part II, Ch. 3, Addison-Wesley, London.
48 Cotton, T.M. and Van Duyne R.P. (1981) J. Am. Chem. Soc. 103, 6020–6026.
49 Lutz, M. and Brown, J.S. (1977) Biochim. Biophys. Acta 460, 408–430.
50 Gouterman, M. (1978) in The Porphyrins (Dolphin, D., ed.), Vol. III, Ch. 1, Academic Press, New York.
51 Woodbury, W.T. and Parson, W.W. (1984) Biochim. Biophys. Acta 767, 345–361.
52 Arata, H. and Parson, W.W. (1981) Biochim. Biophys. Acta 638, 201–209.
53 Deisenhofer, J., Epp, O., Miki, K., Huber, R. and Michel, H. (1984) J. Mol. Biol. 180, 385–398.
54 Kestner, N.R., Logan, J. and Jortner, J. (1974) J. Chem. Phys. 52, 6272–6791.

55 Fajer, J., Brune, D.C., Davis, M.S., Forman, A. and Spaulding, L.D. (1975) Proc. Natl. Acad. Sci. USA 72, 4956–4960.
56 Davis, M.S., Forman, A. and Fajer, J. (1979) Proc. Natl. Acad. Sci. USA 76, 4170–4174.
57 Fajer, J., Davis, M.S., Brune, D.C., Spaulding, L.D., Borg, D.C. and Forman, A. (1977) Brookhaven Symp. Biol. 28, 74–103.
58 Kleinfeld, D., Okamura, M.Y. and Feher, G. (1985) Biochim. Biophys. Acta, in the press.
59 Agmon, N. and Hopfield, J.J. (1983) J. Chem. Phys. 79, 2042–2053.